

Cylinder Vibration Resulting from Switching of Shear Layer Separated from an Upstream Cylinder

Md. Mahbub Alam¹, Y. Zhou^{1,2}, H.L. Cao¹ and P. Zhang²

¹Department of Mechanical Engineering and Automation
 Shenzhen Graduate School, Harbin Institute of Technology, Shenzhen, China

²Department of Mechanical Engineering
 The Hong Kong Polytechnic University, Hong Kong

Abstract

Free vibrations are examined of a cantilever-supported circular cylinder of diameter D placed behind another of smaller diameter d . The diameter ratio d/D is 0.24 ~ 1.00 and cylinder spacing L/d is 1 ~ 2, where L is the distance between the centre of the upstream cylinder to the forward stagnation point of the downstream cylinder. An unusual violent vibration was observed at $d/D = 0.24 \sim 0.8$ for $L/d = 1$ or $d/D = 0.24 \sim 0.6$ for $L/d = 2$. It is proposed that, at a small d/D , the upstream cylinder wake narrows, and the shear-layer reattachment position on the downstream cylinder approaches the forward stagnation point, and hence the high-speed slice of the shear layer could impinge upon alternately the two sides of the cylinder, thus exciting the downstream cylinder. The violent vibration occurs at a reduced velocity $U_r (= U_\infty D/f_n)$, where U_∞ is the free-stream velocity and f_n is the natural frequency of the fluid-structure system associated with the downstream cylinder $\approx 13\text{--}22.5$, depending on d/D and L/d , and grows rapidly for a higher U_r . It is further noted that the flow behind the downstream cylinder is characterized by two predominant frequencies, corresponding to the cylinder vibration frequency and the natural frequency of vortex shedding from the downstream cylinder, respectively. While the former persists downstream, the latter vanishes rapidly.

Introduction

Bokaian & Geoola [1] investigated the case of two identical cylinders where the upstream cylinder is fixed and the downstream one is both-end-spring-mounted, allowing both ends to vibrate at the same amplitude (i.e., two-dimensional model) and in the cross-flow direction only. The investigated ranges of spacing ratio between the cylinders L/d , reduced velocity $U_r (= U_\infty D/f_n)$ and Reynolds number $Re (= U_\infty D/\nu)$ were 0.59~4.5, 3.8~10, 600~6000, where U_∞ is the free-stream velocity, ν is kinematic viscosity of fluid, and f_n is natural frequency of the cylinder system; see Fig. 1 for the definitions of d , D and L . Depending on L/d , the cylinder exhibited only galloping ($L/d = 0.59$), or only vortex resonance ($L/d > 2.5$) or a combined vortex-resonance and galloping ($L/d = 1.0$), or a separated vortex excitation (VE) and galloping ($1.5 \leq L/d \leq 2.5$). Bokaian & Geoola [2] almost at the same L/d , U_r and Re ranges investigated the other case where the downstream cylinder is fixed and the upstream one is both-end-spring-mounted. They reported both galloping and vortex-resonance vibration generated for $L/d \leq 1.25$ and $1.25 < L/d < 4.5$, respectively. For both VE and galloping, vortex shedding frequency f_v was found to lock-on to vibration frequency. Note that the vibration always occurs at f_n . The VE corresponds to vibration occurring near U_r where the natural vortex shedding frequency is close to f_n , and the galloping vibrations persist for higher U_r corresponding to a higher natural vortex shedding frequency than f_n . The mass-damping parameter

$m^*\zeta$ was 0.018~0.2, where m^* is the mass ratio and ζ is the damping ratio. Brika and Laneville [3-4] investigated response of the downstream cylinder with the upstream cylinder stationary or vibrating, for $L/d = 6.5 \sim 24.5$, $U_r = 4 \sim 21$ ($Re = 5.1 \times 10^3 \sim 2.75 \times 10^4$). The system had a very low $m^*\zeta$ of 0.00007. When the upstream cylinder was stationary, the response of the downstream cylinder was no more hysteretic and it was strongly dependent on L/d ; VE regime became wider and shifted to lower U_r with increasing L/d . For $L/d = 6.5 \sim 8$, the cylinder exhibited a combination of VE and galloping. Hover & Triantafyllou [5] examined response of and forces on the spring-mounted downstream cylinder for $L/d = 4.25$. They observed both VE and galloping to occur when U_r was varied from 2 to 17, with changing f_n at constant U_∞ corresponding to $Re = 3.05 \times 10^4$. There are some other studies concerning flow-induced forces on two tandem fixed cylinders (e.g., [6]) and flow characteristics over the two cylinders vibrated forcibly in in-phase and out-of-phase modes (e.g., [7]).

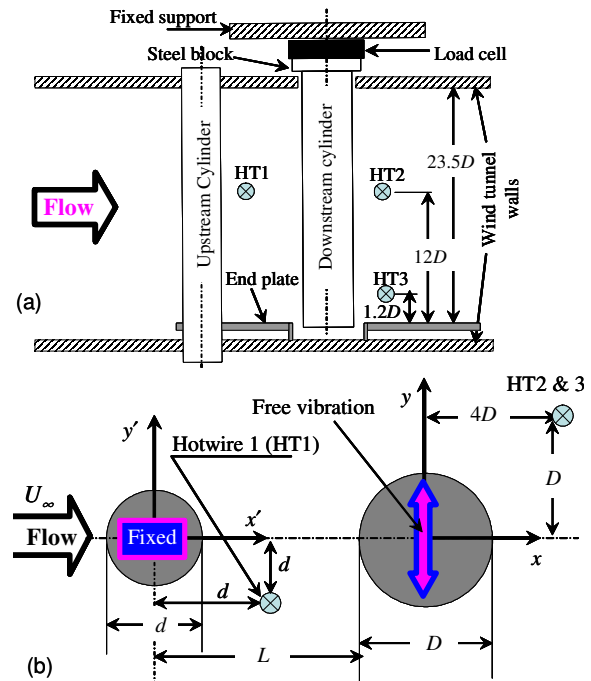


Fig. 1. (a) experimental setup, (b) definitions of symbols

This work aims to study experimentally flow-induced response of a cantilever circular cylinder at a high $m^*\zeta (=3.95)$ value in the presence of an upstream cylinder of different diameters. The free

end of the cantilever cylinder is free to move in two degrees of freedom. The upstream cylinder diameter (d) is varied, with the downstream cylinder diameter (D) unchanged, so that the ratio d/D varies from 1.0 to 0.24. Two $L/d = 1.0$ and 2.0 are considered, and they are within the reattachment regime. The flow-induced responses A_x and A_y in the x - and y -direction (where A stands for amplitude of vibration at the free-end of the cylinder) and cylinder vibration frequency are systematically measured for $U_r = 0.8 \sim 32$. Furthermore, f_v behind the downstream cylinder and in the gap between the cylinders are examined.

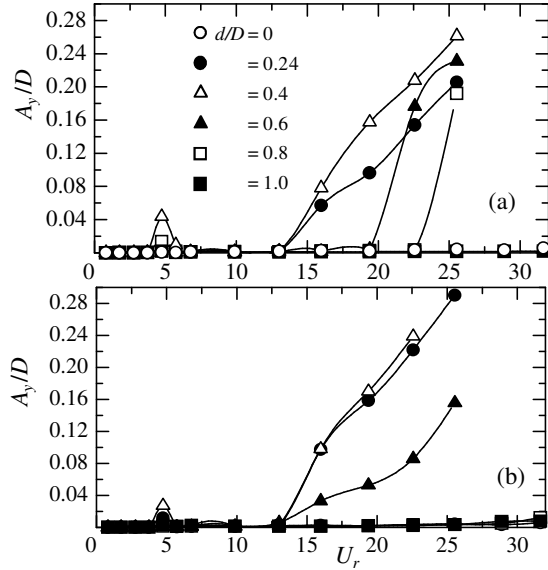


Fig. 2. Vibration amplitude A_y/D at (a) $L/d = 1$, (b) $L/d = 2$.

Experimental details

Measurements were conducted in a low-speed, close-circuit wind tunnel with a 2.4-m-long test section of 0.60 m \times 0.60 m. Figure 1 shows schematically experimental setup and the definitions of coordinates (x' , y' , z') and (x , y , z), with the origins defined at the upstream and downstream cylinder centers at the mid-span, respectively; the x' - and x -axis are along the free stream direction, the y' - and y -axis are perpendicular to the x -axis in the horizontal plane and the z' - and z -axis are normal to both x and y , following the right-hand system. All cylinders were made of brass. The upstream cylinder was solid and fixed-mounted at both ends, inserting through the same diameter hole of 30 mm length at the wind tunnel walls. On the other hand, the downstream cylinder of outer diameter $D = 25$ mm was hollow, inner diameter 21 mm, 700 mm in length, and cantilever-mounted on an external rigid support detached from the wind-tunnel wall. To avoid further interference/complexities by cylinder free-edge vortex, an end plate was used. The free end of cylinder was just into the hole of end plates (Fig. 1a). The size of the hole on the end plate was $2D$, ensuring enough clearance to allow the cylinder to undergo vibrations. The active span of the cylinder, exposed in the wind tunnel is $23.5D$ (587 mm). d was 25, 20, 15, 10 and 6 mm, respectively, and the corresponding d/D was 1.0 \sim 0.24, resulting in a maximum blockage of about 2.4%, and a minimum aspect ratio of 23.5. U_∞ was varied from 0.5 to 20 m/s, corresponding to variation of U_r from 0.8 to 32, Reynolds numbers (Re) of 825 to 3.3×10^4 based on the downstream cylinder. The cylinder corresponded to first, second

and third modes natural frequency $f_{n1} = 24.9$, $f_{n2} = 159.8$ and $f_{n3} = 364$ Hz, respectively.

Three tungsten wires of 5 μ m in diameter and approximately 2 mm in length, one (HW1) placed at (x'/d , y'/d , z'/d) = (1, -1, 0), and the other two (HW2 and HW2) placed at (x/D , y/D , z/D) = (4, 1, 0) and (4, 1, 10.55), respectively (Fig. 1). They were used to measure the frequencies of vortex shedding from the cylinders. Free end vibration displacement of the cylinder was measured by using a standard laser vibrometer. A PIV system was used for flow visualization.

Presentation of results and discussion

Response characteristics

Normalized vibration amplitudes A_y/D at $L/d = 1$ and 2 are presented in Fig. 2. The horizontal axis U_r is based on f_{n1} . The figures also include the data for a single isolated cylinder ($d/D = 0$). First at $L/d = 1$, violent vibration is unveiled at $d/D = 0.24$, 0.4, 0.6 and 0.8 for $U_r > 13$, 13, 19.5 and 22.5, respectively in addition to a visible VE at around $U_r = 4.75$ for $d/D = 0.24$ and 0.4. For the vibration generated cases $d/D = 0.24 \sim 0.8$, the starting U_r of vibration generation is lower for a lower d/D , implying that a decreasing d/D anyhow causes a higher instability of flow and/or an increase of negative damping on the cylinder. At $L/d = 2$, vibration is generated at $d/D = 0.24 \sim 0.6$ for $U_r > 13$, this d/D range is smaller than that at $L/d = 1$. Hence it can be conferred that a cantilevered cylinder submerged in the wake of another may experience catastrophic vibration. In addition, a decreasing d/D is prone to generate violent vibration, which is reverse in the sense that a small cylinder placed upstream of a large cylinder may weaken forces on and vortex shedding from the large cylinder.

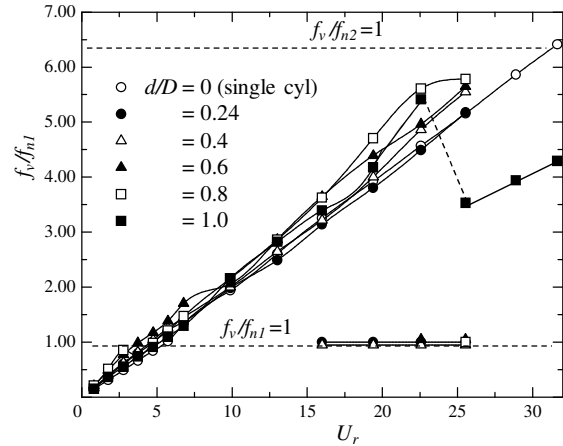


Fig. 3. Variation of f_v/f_{n1} at $L/d = 1$.

Wake evolution

Figure 3 shows f_v/f_{n1} at $L/d = 1$ where f_v was obtained from power spectral analysis of HW2 signal. f_v/f_{n1} closes to 1 at about $U_r = 4.75$, consistent with the existent of a small peak at the same U_r in $A_y/D-U_r$ plot (Fig. 2). At $d/D = 0$, f_v/f_{n1} increases linearly and reaches $f_v/f_{n2} = 1$ at $U_r = 32$. f_v/f_{n1} for other d/D also climbs monotonically except for $d/D = 1$ which displayed a sudden drop between $U_r = 22.6$ and 25.5, marked by a dashed line. Note that f_v/f_{n1} for this d/D corresponds to a Strouhal number of about 0.2 for $U_r \leq 22.6$ ($Re \leq 2.34 \times 10^4$) and 0.14 for $U_r \geq 25.5$ ($Re \geq 2.65 \times 10^4$). The flow structures in the two ranges of U_r are characterized by the two shear layers emanating from the upstream cylinder reattach steadily on downstream side of the

downstream cylinder for $U_r \leq 22.6$, and those reattach alternately on the upstream side for $U_r \geq 25.5$. At $d/D = 0.24, 0.4, 0.6$ and 0.8 for $U_r \geq 16, 16, 19.5$ and 22.5 , respectively where vibration is generated, another frequency at $f_n/f_{nl} = 1$ was observed as presented in the figure. The existence of this frequency may result from either large scale vortex shedding at f_{nl} or perturbation by the cylinder vibration. As the cylinder is cantilevered, its vibration amplitude is maximum at the free end and minimum (negligibly small) at the base; hence there should be a significant spanwise variation of vortex shedding. Typical power spectrum results of streamwise velocity at $d/D = 0.4, L/d = 1, U_r = 19.9$ are presented in Fig. 4, showing how vortex shedding vary along the span of the cylinder and how the wake evolve along the downstream. Two peaks are observed in the power spectrum results of hotwire at the free end (Fig. 4a), corresponding to natural vortex shedding frequency and f_{nl} , respectively. While the peak at the natural vortex shedding frequency wanes as x/D increases, that at f_{nl} grows. The observation implies that, when galloping vibration is generated, the shear layers shed vortices at the natural vortex shedding frequency, and the wake significantly oscillates at f_{nl} . Presumably the wake oscillation amplitude grows along the downstream, distorting and/or weakening the convective vortices of the natural-vortex-shedding frequency. Thus the peak heights at the natural vortex shedding frequency and f_{nl} tumble and enlarge, respectively as x/D increases. Similar observation is made in the results at the mid-span of the cylinder. At the base of the cylinder where vibration amplitude is negligible, peak at f_{nl} disappears.

Modes of vibration

Figure 5 displays vibration characteristics in one period of the galloping vibration (a-d) and VE (e). Galloping vibration occurs mainly in the first mode of vibration in the cross-stream direction (Fig. 5a), while the second mode of vibration also exists in the streamwise direction (Fig. 5b). The vibration signal was decomposed into the first and second modes, and the trajectories of the cylinder corresponding to the two modes were obtained, as presented in Fig. 5(b, c). VE vibration trajectory (Fig. 5e) is however different from the galloping.

Instability generation mechanism

When both cylinders are fixed (Fig. 6a), the two shear layers emanating from the upstream cylinder reattach steadily on the downstream cylinder. The thickness of a shear layer can be divided into three slices: highly turbulent slice, high velocity slice and nearly free-stream slice. Vibration for two tandem cylinders mainly results from the switching instability of the shear layers originated from the upstream cylinder, as sketched in Fig. 6(b). The switching instability is generated from whether the high velocity slice of a shear layer passes on the same side (up?) or opposite side (down?) of the downstream cylinder. The high velocity slice generates highly negative pressure on the surface over which it goes [8]. Now let us discuss the physics of flow on the vibrating cylinder. When the cylinder is moving upward from its centerline (Figs. 6c, d), the high velocity slice of the upper shear layer goes on the upper side and causes an upward lift force to pull the cylinder upward. On the other hand, when the cylinder is moving down (Figs. 6e, f), toward the centerline, the high velocity slice of the same shear layer sweeps the lower side; hence a downward lift force is generated to pull the cylinder toward the centerline. Similarly, the next half cycle is associated with the lower shear layer. Previous sections proved that a smaller d/D is more prone to generate vibration. Why? As d/D tends to be small, the upstream cylinder wake narrows, and the shear-layer reattachment position on the downstream cylinder moves to the front stagnation point. Hence the shear layer is more

prone to switch and results in the vibration. If the upstream cylinder is larger than or equal to the downstream one, i.e., $d/D \geq 1$, the upstream wake becomes wider, and the shear layers get enough stability to pass over the respective side of the downstream cylinder, hence no vibration is generated.

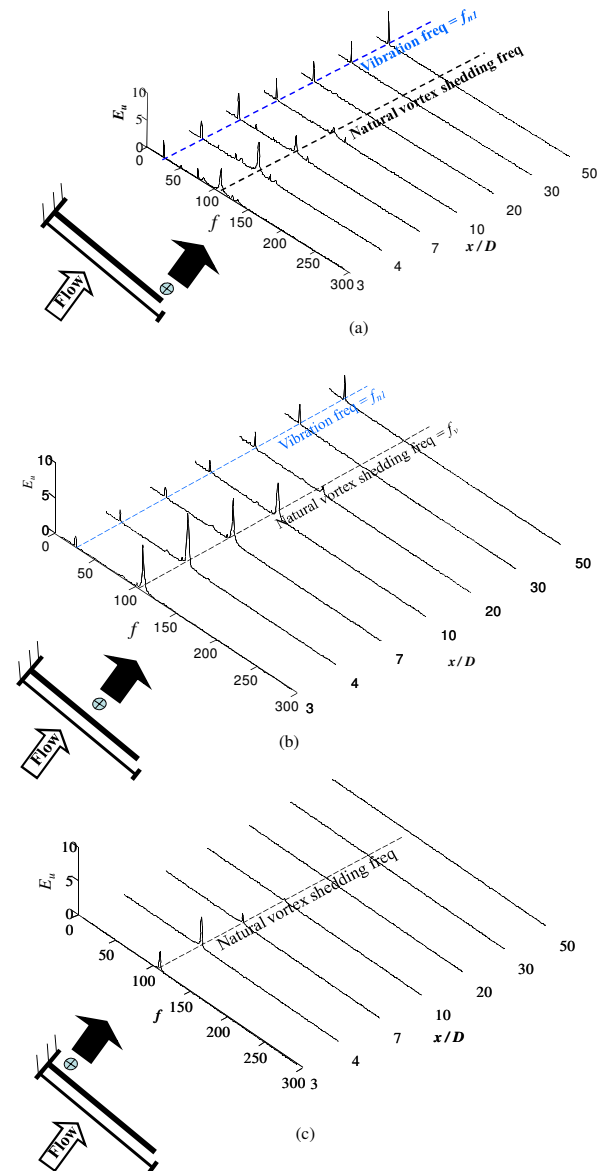


Fig. 4. Power spectrum of streamwise velocity at $d/D = 0.4, L/d = 1, U_r = 19.9$ for hotwire at the (a) free-end ($z/D = 10.55$), (b) mid-span ($z/D = 0$), (c) base ($z/D = -10.55$).

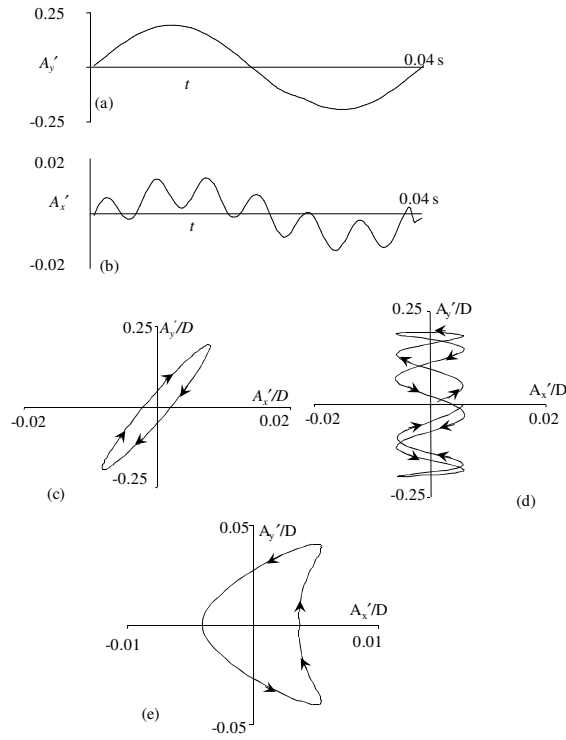


Fig. 5. $d/D = 0.4$, $L/d = 1$. (a, b) Instantaneous displacement of the cylinder in y and x directions, respectively; (c, d) trajectories of the cylinder in the first and second modes of vibration., respectively; $U_r = 22.5$. (e) Trajectory of the cylinder at VE, $U_r = 4.75$.

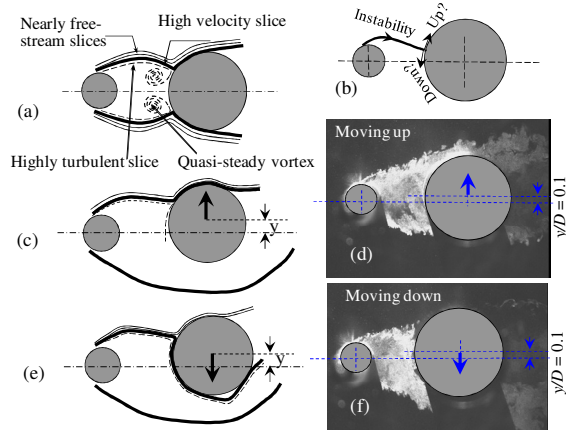


Fig. 6. Flow structure generating galloping. (a) No vibration: steady-reattachment flow. (b) Instability generation. For a given displacement, visualized flow ($d/D = 0.4$, $L/d = 2$, $U_r = 19.9$) and sketch when cylinder moving (c, d) upward, (e, f) downward..

Conclusions

The preliminary investigation leads to following conclusions.

- (i) Vortex-excited vibration occurs for $d/D = 0.24$ and 0.4 at resonance $U_r \approx 4.75$ and is suppressed for $d/D \geq 0.6$ and $d/D = 0$. In addition, a violent divergent lateral structural vibration is observed at $d/D = 0.24 \sim 0.8$ for $L/d = 1$ and at $d/D = 0.24 \sim 0.6$ for $L/d = 2$. The smaller d/D , the narrower is the wake in the gap of the cylinders and the lower is U_r , at which the violent vibration occurs. For example, this U_r is 13, 13, 19.5 and 22.5 for $d/D = 0.24, 0.4, 0.6$ and 0.8 , respectively, for $L/d = 1$.
- (ii) While the vibration in the lateral direction occurs dominantly at the first-mode natural frequency, that in the streamwise direction happens at both first- and second-mode natural frequencies.
- (iii) Two predominant frequencies in the wake were identified, associated with natural vortex shedding and the vibration of the cylinder, respectively. While the vortices associated with the natural vortex shedding frequency decay rapidly, those associated with the vibration frequency persist in the downstream.
- (iv) The possible mechanism of the violent vibration is that the upstream cylinder wake narrows with decreasing d/D , and the shear-layer reattachment position on the downstream cylinder approaches the forward stagnation point. As a result, the high-speed slice of the shear layer could impinge upon alternately on the two sides of the cylinder, thus getting it excited.

References

- [1] Bokaian, A. & Geoola, F., 1984, Wake-Induced Galloping of Two Interfering Circular Cylinders, *J. Fluid Mech.*, 146, 383-415.
- [2] Bokaian, A., & Geoola, F., 1984, Proximity-Induced Galloping of Two Interfering Circular Cylinders, *J. Fluid Mech.*, 146, 417-449.
- [3] Brika, D. & Laneville, A., 1997, Vortex-Induced Oscillations of Two Flexible Circular Cylinders Coupled Mechanically, *J. Wind Eng. Indust. Aerodyn.*, 69-71, 293-302.
- [4] Brika, D. & Laneville, A., 1999, The Flow Interaction between a Stationery Cylinder and a Downstream Flexible Cylinder, *J. Fluids Struct.*, 13, 579-606.
- [5] Hover, F.S. & Triantafyllou, M.S., 2001, Galloping Response of a Cylinder with Upstream Wake Interference, *J. Fluids Struct.*, 15, 503-512.
- [6] Alam, M.M, Moriya, M., Takai, K. & Sakamoto, H., 2003, Fluctuating Fluid Forces Acting on Two Circular Cylinders in a Tandem Arrangement at a Subcritical Reynolds Number", *J. Wind Eng. Indust. Aerodyn.*, 91, 139-154.
- [7] Mahir, N. & Rockwell, D., 1996, Vortex Formation from a Forced System of Two Cylinders, Part I: Tandem Arrangement, *J. Fluids Struct.*, 10, 473-490.
- [8] Alam, M. M., Sakamoto H. & Zhou, Y., 2005, Determination of Flow Configurations and Fluid Forces acting on Two Staggered Circular Cylinders of Equal Diameter in Cross-Flow, *J. Fluids Struct.*, 21, 363-394.